JOURNAL OF SPACECRAFT AND ROCKETS
Vol. 34, No. 3, May–June 1997

Comparison Between Numerical and Experimental Results on Different Hermes Elevon Shapes

F. De Filippis,* M. Serpico,† and M. Marini†
Centro Italiano Ricerche Aerospaziali, 81043 Capua (CE), Italy
and
J. P. Tribot‡ and M. Ravachol§
Dassault Aviation, 92552 St. Cloud Cedex, France

A comparison between experimental and numerical data around two-dimensional deflected Hermes elevon configurations, in wind-tunnel conditions, is discussed. The available experimental data are compared with the numerical results obtained with different state-of-the-art hypersonic Navier–Stokes codes to make a code-code and a code-experiments verification. The main physical parameters characterizing the shock-wave/boundary-layer interaction that occurs around the hinge in the considered flowfields, as well as separation, laminar–turbulent transition, and peak heating, have been analyzed and verified by means of some theoretical-empirical correlation laws. The present experimental results have been obtained in the frame of an European Space Agency program.

Nomenclature

C^*	= Chapman–Rubesin constant
h	= heat transfer
M	= Mach number
n	= exponent for peak heating correlation
p	= pressure
Re	= Reynolds number
X	= X coordinate
Y	= Y coordinate
α, β	= constants for Eq. (1)
ρ	= density
θ	= deviation angle

Subscripts

e	= edge of boundary layer
is	= incipient separation
l	= laminar conditions
pk	= peak value
ref	= reference value
t	= turbulent conditions
ui	= upstream of interaction
w	= wall

Introduction

DURING the activities for designing the Hermes re-entry vehicle, experimental measurements in wind-tunnel conditions (S4ma hypersonic facility at the ONERA Modane Test Centre) have been carried out on a reduced scale (1/40) model.

In particular, wall heat flux distributions have been measured over two different Hermes models with two elevon shapes (half-cambered and full-cambered, as shown in Fig. 1), and have been obtained by using two different techniques, thermocolor (TC) and thermocouples (TCP), with natural laminar to turbulence transition and imposed transition by means of wires fixed on the model.

Presented as Paper 96-2472 at the AIAA 14th Applied Aerodynamics Conference, New Orleans, LA, June 18–20, 1996; received Oct. 7, 1996; revision received Feb. 11, 1997; accepted for publication Feb. 14, 1997.

*Research Scientist, Aerothermodynamics Department, Via Maiorise. Member AIAA.
†Research Scientist, Aerothermodynamics Department, Via Maiorise.
‡Aerospace Engineer, Theoretical Aerodynamics, 78 Quai Marcel Dassault. Member AIAA.
§Research Scientist, Theoretical Aerodynamics, 78 Quai Marcel Dassault. Member AIAA.

The numerical simulations have been carried out by using two different Navier–Stokes hypersonic codes: 1) VG2DB, the two-dimensional version of VIRGINI three-dimensional code, intensively used during the Hermes program, which uses a finite element approach on unstructured grids, developed by Dassault Aviation and 2) H2NS, a two-dimensional and/or axisymmetric code that uses a finite volume technique on structured grids, developed by the Centro Italiano Ricerche Aerospaziali (CIRA).

The flat-, half-, and full-cambered shapes (see Fig. 1) of the elevon have been studied to assess the influence of the geometric shape on the shock-wave/boundary-layer interaction and laminar to turbulence transition. In fact, a critical issue of these numerical simulations is to correctly set the transition onset from laminar to turbulent flow and to choose the more appropriate turbulence model to match experimental results. Two different turbulence models have been considered: an algebraic one implemented in H2NS and the two-equation k–ϵ one implemented in the VG2DB code.

Zonal Navier–Stokes computations have been carried out taking into account the Hermes elevon region. The computational domain has been created by zooming on the elevon region of the Hermes bottom and extends from $X = 194.35$ mm to the end of the control surface ($X = 395$ mm for the flat elevon), as shown in Fig. 1; the two-dimensional section has been selected at a spanwise coordinate equal to 2000/40 mm from the centerline. At the inlet boundary of the computational domain, the flow variables previously calculated by an Euler equilibrium flow approach coupled with a laminar boundary-layer assumption on the global vehicle configuration have been enforced (postshock conditions) as a viscous prediction to start Navier–Stokes computations.

Reservoir conditions of the facility S4ma, freestream conditions inside the test chamber, and local (inlet) conditions for the computational domain are as follows. For the reservoir conditions, the total pressure is 85 bars and total temperature is 1100 K. For the test chamber conditions (at the nozzle exit), the Mach number is 9.90, the unit Reynolds number is 2.1×10^6/m, the angle of attack is 30 deg, the elevon deflection is 10 deg, and the model scale is 1/40. At the local inlet conditions ($X = 194.35$ mm), the Mach number is 2.034, the unit Reynolds number is 1.404×10^6/m, the wall temperature is 290 K, the temperature is 603 K, the pressure is 7432.5 Pa, the density is 0.0427 kg/m^3, and the specific heats ratio γ is 1.392.

Two kinds of shock-wave/boundary-layer interactions have been selected: laminar–turbulent, with transition onset around the hinge of the elevon, and turbulent–turbulent, with transition onset not far from the inflow section. The computational test matrix is reported in Table 1, where the available heat flux measurements are also indicated.

In Table 1 natural transition stands for transition onset downstream of the hinge ($X = 347.65$–349.75 mm for VG2DB and set to $X = 348.7$ mm for H2NS), forced transition stands for transition onset near the inlet of the computational domain ($X = 200$–205 mm for VG2DB and set to $X = 202.5$ mm for H2NS) and large transition stands for a transition region extended between two different stations by means of an intermittency function.

The half-cambered elevon shape was related to the Hermes version 314 and the full-cambered shape to the Hermes version 1.0, whereas the flat elevon shape has to be considered as a reference shape for which experimental model and data are not available. For all of the geometric configurations two simulations have been performed by considering, respectively, transition at hinge and fully turbulent flow and a laminar computation has been added as a reference for flat- and half-cambered shapes. An additional run has been added for the full-cambered shape (computed only with VG2DB, simulating a large transition region around the hinge). All of the computations have been performed by using a mesh (153×129 grid points) stretched in the direction perpendicular to the wall to correctly predict the boundary layer. The structured grid is characterized by a minimum normal spacing in proximity of the corner equal to 7.5 μm (and a corresponding aspect ratio equal to about 190). An unstructured grid with the same number of grid points has been used for VG2DB numerical simulations.

Experimental Facility and Results

Experimental results are available in the S4ma hypersonic wind tunnel facility,[1,2] in which since 1987 a great number of tests have been performed in the frame of the Hermes program. S4ma is a blow-down wind tunnel fed with air from the center's compressed air store (109 m^3 at a pressure of 270 bar). A heater, which is 2 m in diameter and 10 m high and contains 11 tons of alumina pebbles, can be raised by propane combustion to a maximum temperature of 1850 K. The wind tunnel is equipped with three nozzles where the Mach number at the exit section (test chamber) ranges from 6.4 to 12. The core diameter is 0.55 m, providing for tests with model lengths of 0.35 m at an angle of attack up to 50 deg and a model span of 0.23 m that can be conducted for run durations between 20 and 60 s. The test chamber is cubic (3-m-long sides) and is equipped with an angle-of-attack table ($\pm$15 deg, rotating at 2–5 deg/s) and sideslip table ($\pm$50 deg, at a speed of 2.8–11 deg/s). A 128-channel data acquisition system is available, 92 of which can be used for heat flux measurements, processed in real time on a VAX 6320 computer. A great number of six-component balances (for force and moment measurements) and a shadowgraph system (with a field of 800 mm) are also available.

Table 1 Test matrix

Shape	Flow	H2NS	VG2DB	Exp. Tech.
Flat	Laminar	X	X	
Flat	Natural Transition	X	X	
Flat	Forced Transition	X	X	
Half	Laminar	X	X	
Half	Natural Transition	X	X	TC, TCP
Half	Forced Transition	X	X	TC
Full	Natural Transition	X	X	TC, TCP
Full	Large Transition		X	TC, TCP
Full	Forced Transition	X	X	

The experimental results for the Hermes model in the S4ma wind tunnel are available for two Hermes elevon shapes[1,2]: half-cambered shape (Hermes version 314) and full-cambered shape (Hermes version 1.0).

These data have been obtained by using two different techniques: TC and TCP. The experimental uncertainty is about 20% for the TC technique and 10% for the TCP technique. For the half-cambered elevon shape a set of measurements data with forced transition is also available. The transition of the boundary layer is promoted by means of two ring lines located near the nose of the model. All of the experimental data are reported in Figs. 2 and 3. The heat flux is normalized with a reference value of 280 kW/m^2, which is the heat flux value calculated by means of the Fay–Riddel formula on a sphere in wind-tunnel conditions, characterized by a 1 m radius of curvature, reduced to the scale model (1/40).

The experimental results obtained with the two different measurement techniques do not show good agreement. The main discrepancies are observed on the heat flux level downstream of the interaction, where the laminar to turbulence transition occurs. This fact has to be ascribed to the different material of the solid surface (metallic for TCP and insulated for TC), which affects the transition on the elevon surface by means of temperature in the proximity of the wall (however, in the wind-tunnel conditions a transitional heat flux peak is observed, and so the turbulent computation could not reflect the true physics of the phenomenon).

Numerical Methodologies

The numerical two-dimensional simulations have been performed in the assumption of laminar, transitional, and turbulent perfect gas flow over three different geometries of the elevon, deflected by 10 deg accordingly to the available experimental data. In the following, a brief description of the main characteristics of the Navier–Stokes hypersonic codes used (VG2DB and H2NS) is reported.

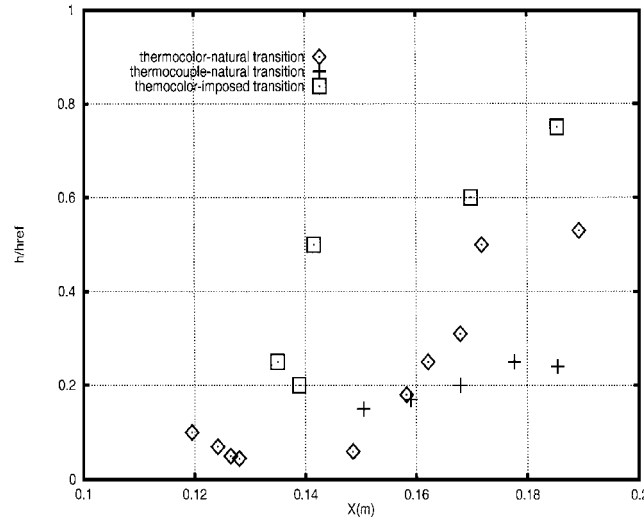

Fig. 2 Experimental heat flux measurements on half-cambered elevon shape.

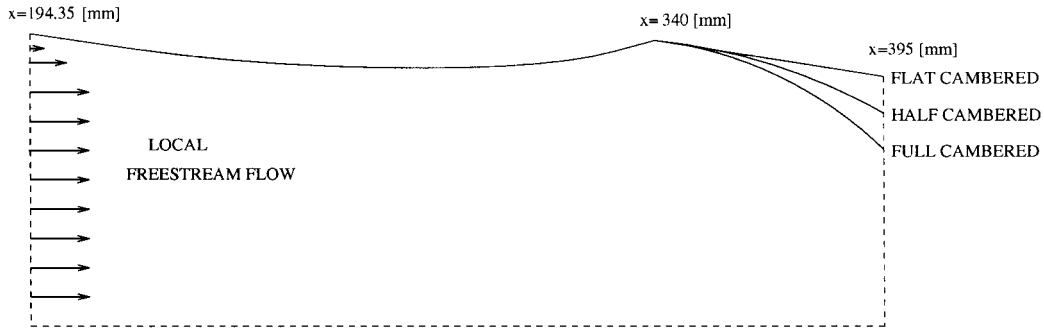

Fig. 1 Flat-, half-, and full-cambered Hermes elevon shapes.

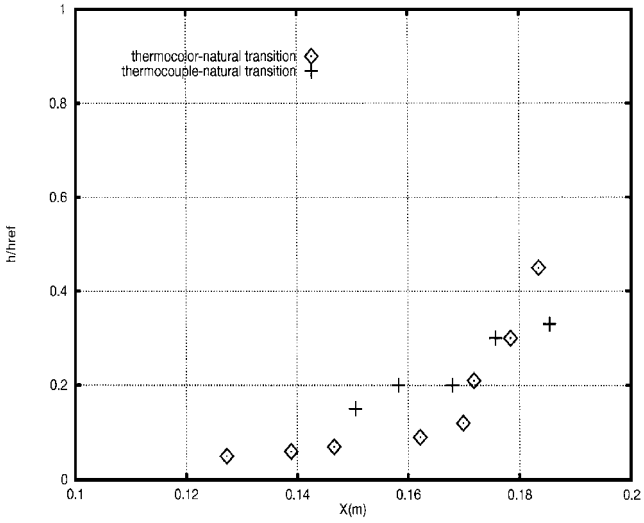

Fig. 3 Experimental heat flux measurements on full-cambered elevon shape.

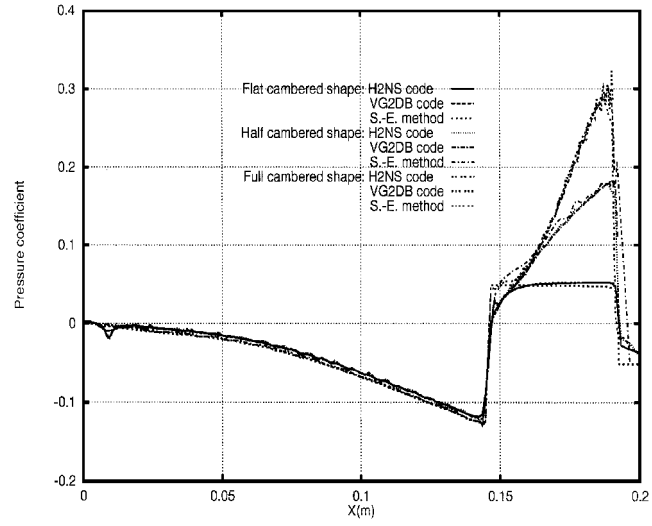

Fig. 4 Numerical-approximate results for the pressure coefficient on different Hermes elevon shapes, fully turbulent case.

VG2DB

The industrial code VG2DB[3,4] uses a finite element approach on unstructured grids. Good stability characteristics and accuracy have been obtained by using the Galerkin least squares (GLS) method. Even though the GLS method is stable, spurious oscillations may occur in the proximity of strong gradients, as well as shock waves and strong expansions. Therefore, a nonlinear discontinuity-capturing operator is added to the formulation. Convergence to a steady solution of the compressible Navier–Stokes equations is achieved by means of an implicit iterative time-marching algorithm. The code is based on a symmetric form of the equations written in terms of entropy variables. Equilibrium chemistry with five-species model of air has been used extensively. Thermochemical nonequilibrium is also available in the code, but it has not been switched on for these simulations. The turbulence model employed is a two-layer model that uses a one-equation model in the viscous sublayer and matches the k–ϵ model in the log-law region. This model has been chosen for its accuracy in predicting high-speed shock-wave/boundary-layer interaction flows. The transition region is extended between two different stations by means of an intermittency function.

H2NS

The research code H2NS solves the full Navier–Stokes equations on structured grids both for internal and external flows, in two-dimensional as well as in axisymmetric cases, with chemical and vibrational nonequilibrium. A finite volume technique has been used, with a flux difference splitting Riemann solver formulation,[5,6] with a second-order reconstruction of fluxes at cell interfaces. A detailed description of this solver is given in Refs. 7–10, where the code has been extensively tested and validated by computing different flowfields as hyperboloid flare, shock–shock type IV interaction, and nozzle flow problems.

Different thermochemical nonequilibrium and transport models are available in the code.[11,12] In the hypothesis of perfect gas, the laminar viscosity has been calculated by means of the Sutherland's law, whereas turbulence effects have been accounted for by modeling the eddy viscosity by means of the algebraic turbulence model of Baldwin and Lomax,[13] in which transition is set to a fixed station.

Discussion of Results

Comparison with Approximate Methods

Initially a comparison of the numerical results with predictions made by using simplified formulations and empirical correlation laws has been made, in particular, concerning the verification of the pressure distribution, the attached or separated boundary-layer character, and the peak heating values. The purpose is to demonstrate if a simplified method based on correlations is able to predict the order of magnitude of heat flux along the elevon. This technique should be useful during a predesign phase.

For the pressure coefficient, the numerical turbulent results have been compared with the ones obtained by using a shock-expansion method. The results relative to the three different cambered shapes are shown in Fig. 4. The good agreement between computational fluid dynamics (CFD) results and simplified shock-expansion results is due to the total absence of recirculating region (numerical computation with fully turbulent flow) and to the thin boundary layer (high Reynolds number flow). As Fig. 4 clearly shows, the effect of the elevon curved shape is a continuous compression that increases the maximum pressure load over the control surface by a factor of about 4 with respect to the flat shape (the deflection is becoming larger, on average).

For the peak heating values, the effects of the geometric curved shape of the body upstream of the hinge have not been accounted for, but an equivalent flat plate compression ramp problem has been analyzed by computing the Mach number at the edge of the incoming boundary layer by means of an inviscid approach (shock-expansion method). Therefore, the Mach number characterizing the shock-wave/boundary-layer interaction is $M_{\mathrm{ui}} \simeq 2.31$, and the effective ramp angle is 10 deg with respect to the flat plate. In these conditions, the incipient separation angle can be calculated[14]:

$$\theta_{\mathrm{is}} = \sqrt{M_{\mathrm{ui}}}\,\alpha \left(\frac{C^*}{Re_{x_{\mathrm{ui}}}} \right)^{\beta} \tag{1}$$

where $Re_{x_{\mathrm{ui}}}$ is the local Reynolds number based on the x coordinate immediately upstream of the interaction, $\alpha = 80$ and $\beta = 0.25$ for laminar boundary-layer conditions, and $\alpha = 42$ and $\beta = 0.086$ for turbulent boundary-layer conditions, whereas $C^* = \sqrt{(\rho_w \mu_w / \rho_e \mu_e)}$. By applying Eq. (1) the incipient separation angle is $\theta_{\mathrm{is}} \simeq 4.6$ deg in laminar conditions and $\theta_{\mathrm{is}} \simeq 20.7$ deg in turbulent conditions, thus fully confirming the laminar and fully turbulent numerical results.

The predicted peak heating has been compared only for flat elevon shapes (on the half- and full-cambered geometries the peak heating cannot be defined due to the curved shape of the elevon), with the empirical correlation laws available in literature, in which the ratio of peak heating to a reference value (upstream of the interaction) is a power of the pressure ratio in the same conditions, i.e.,

$$h_{\mathrm{pk}}/h_{\mathrm{ui}} = (p_{\mathrm{pk}}/p_{\mathrm{ui}})^n \tag{2}$$

where h_{pk} and p_{pk} are the heat transfer peak and the pressure peak measured downstream of the interaction, respectively, and h_{ui} and p_{ui} are the reference quantities, i.e., the heat flux and the pressure values immediately upstream of the interaction. The exponent n ranges from 0.7 to 1.29 in fully laminar conditions and from 0.8

to 0.85 in fully turbulent conditions. Full reference for these different correlations due to Markarian (M), Holden (H), Newmann and Burke (NB), Haslett et al. (HA), and Sayane (S) can be made to the recent work of Simeonides.[15]

In the transitional case, where transition occurs immediately downstream of the hinge thus causing a turbulent peak heating that has to be compared to a laminar reference value, the correlation law is

$$\frac{h_{\mathrm{pk},t}}{h_{\mathrm{ui},l}} = \left(\frac{h_{\mathrm{ui},t}}{h_{\mathrm{ui},l}}\right)\left(\frac{p_{\mathrm{pk}}}{p_{\mathrm{ui}}}\right)^{n_t} \tag{3}$$

The term $(h_{\mathrm{ui},t}/h_{\mathrm{ui},l})$ that accounts for the laminar to turbulence transition has been estimated by numerical values, inasmuch as well-assessed theoretical results of heat flux distributions over curved geometries do not exist.

The obtained results have been reported in Table 2, where H2NS findings are indicated with c1 and VG2DB results are indicated with c2. Markarian uses $n_l = 1.29$ and $n_t = 0.85$, Holden uses $n_l = 0.7$ and $n_t = 0.85$, Newmann and Burke use $n_l = n_t = 0.8$, Haslett et al. use $n_l = 0.75$ and $n_t = 0.8$, and Sayane uses $n_t = 0.8$ (Ref. 15).

In the flat elevon test-case, we conclude that numerical results in terms of $h_{\mathrm{pk}}/h_{\mathrm{ui}}$ through Eqs. (2) and (3) and correlation laws of different authors as found in Ref. 15 seem to show a good agreement in transitional conditions (turbulent peak heating related to a laminar reference value), even though the numerical solutions differ among themselves about 15%, due to the different turbulence modeling, which reflects in the scaling term $(h_{\mathrm{ui},t}/h_{\mathrm{ui},l})$. In fully laminar conditions the discrepancy between numerical results and correlations (with exception of Markarian who uses a much higher exponent) is in average of about 8%, giving rise to a good agreement. Moreover, note the large scattering of data due to the different exponents used. In fully turbulent conditions (turbulent peak heating related to a turbulent reference value), where the scattering of exponent is limited between 0.8 and 0.85, the VG2DB solution shows a very good agreement with correlations (discrepancy of $\pm 1.5\%$), thus confirming the necessity to use a more sophisticated turbulence

Table 2 Peak heating correlation (flat elevon)

	Laminar		Transitional		Turbulent	
	c1	c2	c1	c2	c1	c2
$p_{\mathrm{pk}}/p_{\mathrm{ui}}$	1.529	1.582	1.632	1.633	1.743	1.758
$h_{\mathrm{pk}}/h_{\mathrm{ui}}$	1.265	1.261	5.821	4.333	1.388	1.594
M	1.729	1.807	5.382	4.620	1.604	1.615
H	1.346	1.378	5.382	4.620	1.604	1.615
NB	1.404	1.443	5.252	4.462	1.560	1.570
HA	1.377	1.410	5.252	4.462	1.560	1.570
S			5.252	4.462	1.560	1.570

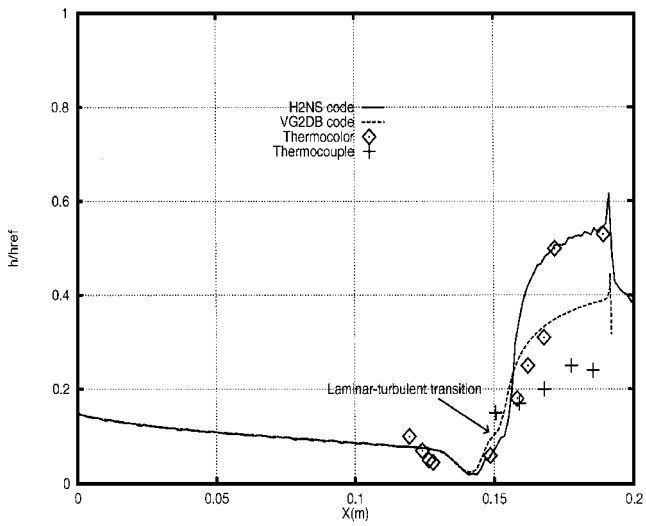

Fig. 5 Normalized heat flux for the half-cambered shape: experiments with natural transition.

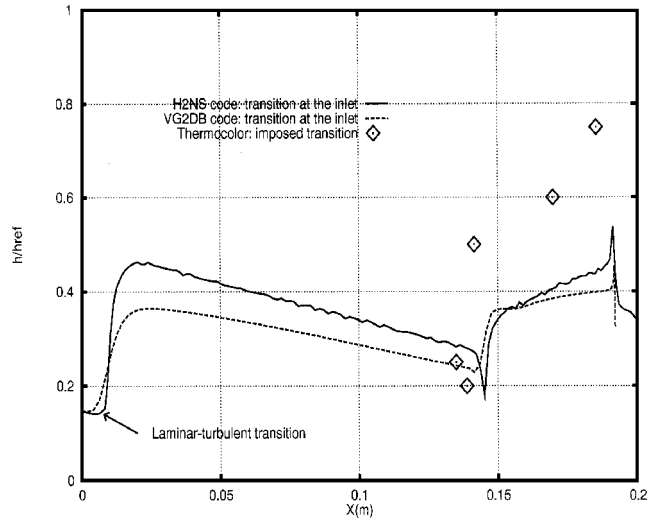

Fig. 6 Normalized heat flux for the half-cambered shape: experiments with imposed transition.

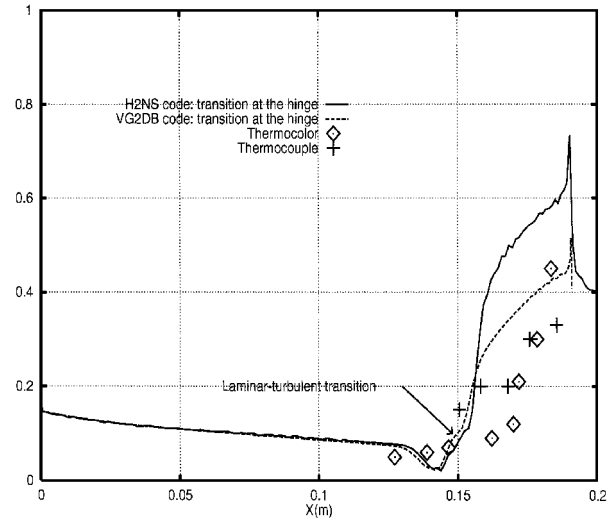

Fig. 7 Normalized heat flux for the full-cambered shape.

modeling (as k–ϵ in VG2DB) with respect to the algebraic one used in H2NS.

Comparison with Experimental Data

In this subsection the numerical–experimental comparison is discussed. The behavior of the flowfield for the different Hermes elevon shapes and for the different laminar–turbulent transition onsets is shown, trying to explain the main differences between numerical and experimental results.

For the half-cambered elevon shape, two sets of experimental data with natural and forced transition are available; the comparison with numerical results is reported in Figs. 5 and 6. The general trend is a quite satisfactory agreement upstream the interaction and a large discrepancy downstream the interaction. This behavior is due to the transitional flow conditions, which produce a laminar–turbulent transition near the reattachment point, and to the three-dimensional effects, which reduce the compression region. The different experimental measurements techniques (TC and TCP) have given different results downstream of the interaction because of the different influence of wall temperature on the transition phenomena. Also, the numerical results obtained with the H2NS and VG2DB codes show different heat flux distributions on the elevon surface and, for fully turbulent cases, over the forebody as well, due to the different turbulence models. The same general behavior is found for the full-cambered elevon shape, whose results are reported in Figs. 7 and 8; in fact, a satisfactory agreement between numerical and experimental results holds only upstream of the interaction. For

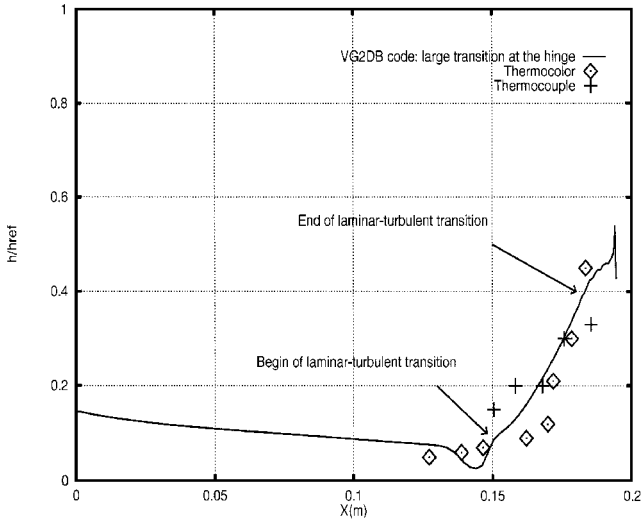

Fig. 8 Normalized heat flux for the full-cambered shape: numerical results with large transition region.

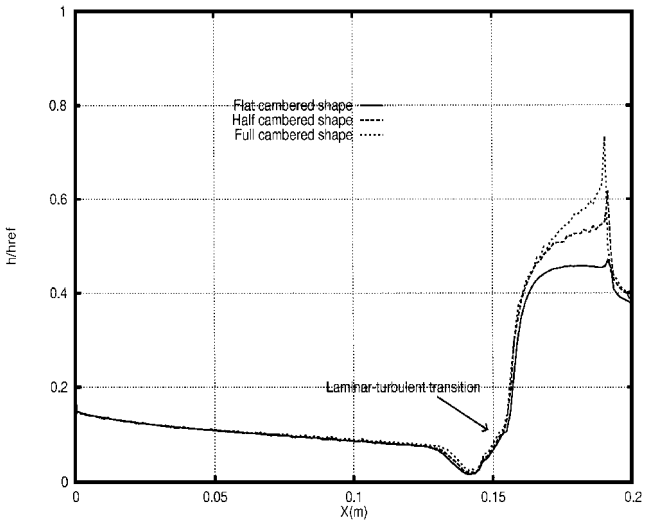

Fig. 9 Normalized heat flux on different Hermes elevon shapes.

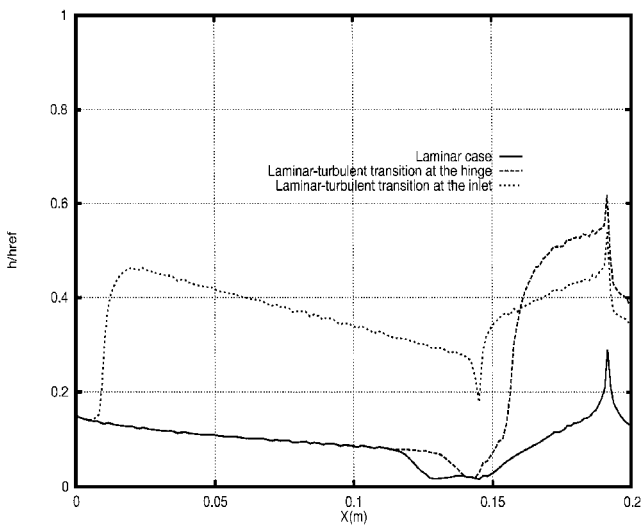

Fig. 10 Normalized heat flux for different laminar–turbulent transition, half-cambered shapes.

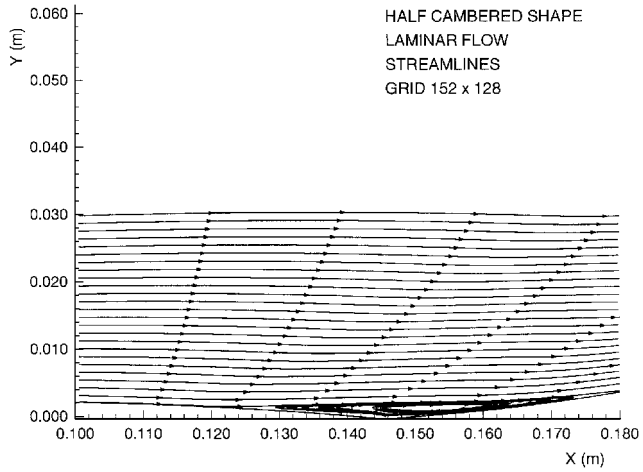

Fig. 11 Streamlines near hinge location for the laminar half-cambered shape.

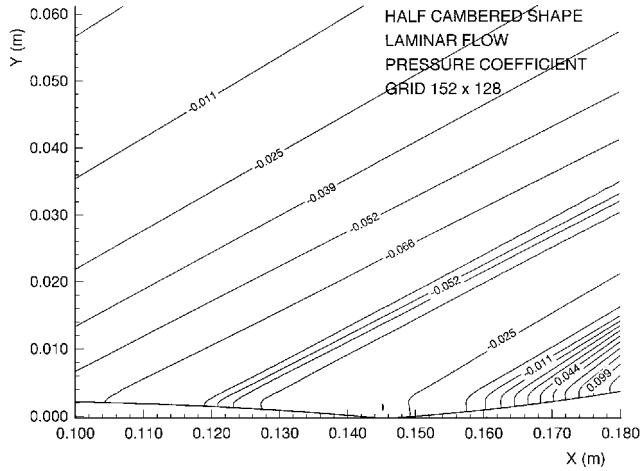

Fig. 12 Isopressure coefficient near hinge location for the laminar half-cambered shape.

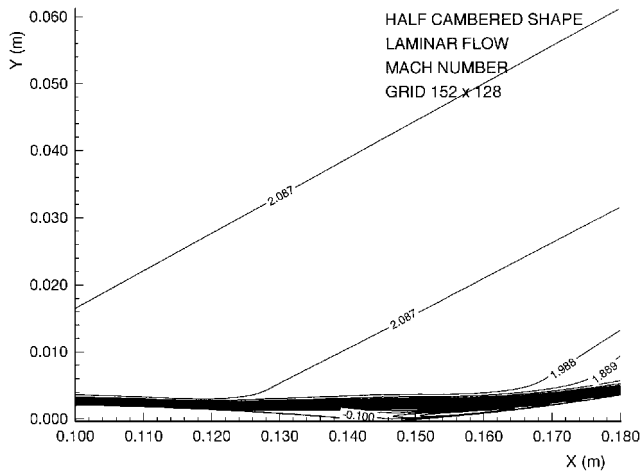

Fig. 13 Iso-Mach lines near hinge location for the laminar half-cambered shape.

the full-cambered elevon shape, a numerical solution, with VG2DB code, assuming an extended transition region has also been computed. The comparison with experimental data (see Fig. 8) also shows a better agreement downstream of the interaction. This last comparison confirms that the main numerical difficulty is not only to select the correct turbulence modeling but also to set the correct laminar–turbulent transition onset. In Fig. 9, the H2NS numerical results with transition located at the hinge, for the three different

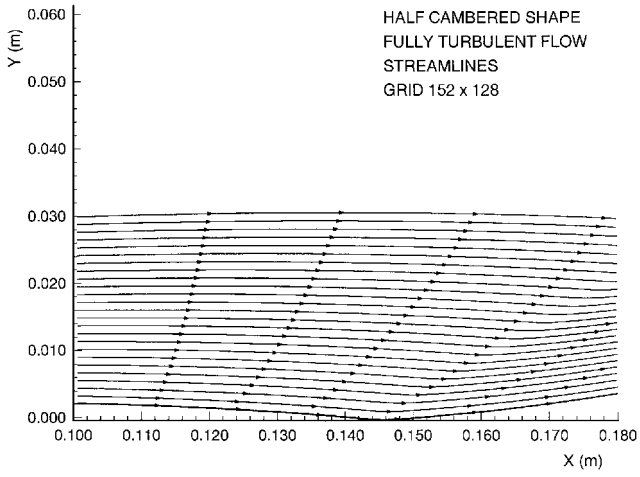

Fig. 14 Streamlines near hinge location for the turbulent half-cambered shape.

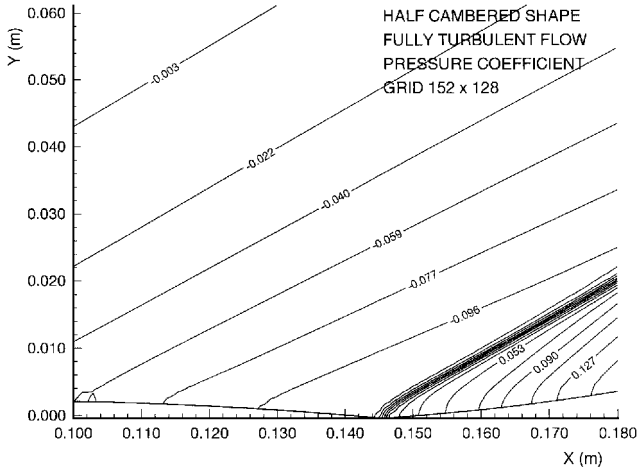

Fig. 15 Isopressure coefficient near hinge location for the turbulent half-cambered shape.

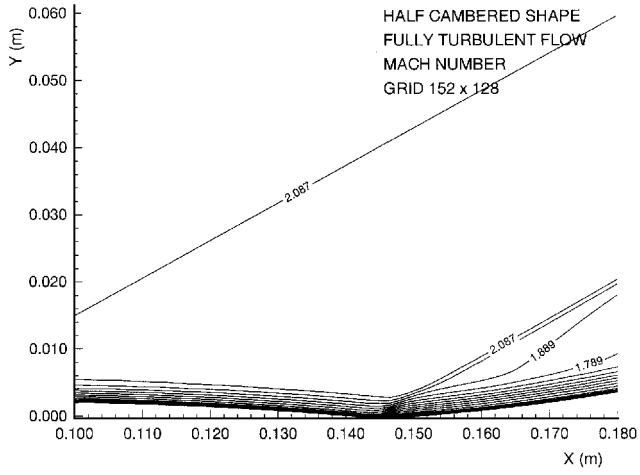

Fig. 16 Iso-Mach lines near hinge location for the turbulent half-cambered shape.

elevon shapes, are shown. The heat flux level increases as the curvature of the cambered shape increases, giving the maximum level for the full-cambered shape, the reason being the continuous flow compression on the curved shape. The influence of the laminar–turbulent transition on the heat flux distribution is shown in Fig. 10, where the maximum heat flux level is predicted by means of H2NS with laminar–turbulent transition located at the reattachment point (hinge location).

The different laminar–turbulent transition location produces a different flowfield, as reported in Figs. 11–16, where the streamlines, the isopressure coefficient, and the iso-Mach contours around the hinge location for the half-cambered shape are shown (computed by means of H2NS code). For laminar flow a recirculating region near the hinge location appears; the separation and recompression shock waves occur in the proximity of the separation and reattachment locations. For turbulent flow the recirculating region disappears, the sonic line is closer to the wall, and a unique sharp shock wave, whose effect is felt more deeply inside the boundary layer with respect to the laminar case, is present at the corner.

Conclusions

A comparison between experimental and numerical data around two-dimensional deflected Hermes elevon configurations, in wind-tunnel conditions, has been discussed. The available experimental data have been compared with the numerical results obtained with VG2DB and H2NS hypersonic Navier–Stokes codes to make a code–code and a code–experiments verification.

The heat flux experimental data, obtained with two different measurement techniques (TC and TCP), differ significantly on the elevon surface, where the laminar to turbulence transition occurs, and this fact has to be ascribed to the different material of the solid surface, which affects transition by means of wall temperature.

A comparison of experimental data and numerical results obtained with simplified formulations, empirical correlation laws, and sophisticated CFD tools has been made. The good agreement between CFD results and a shock-expansion method is due to the absence of recirculation in the fully turbulent case and to the thin boundary layer (high Reynolds number). However, the effect of the elevon curved shape is a continuous flow compression that increases significantly the pressure load over the control surface with respect to the flat shape. By using the peak heating correlation laws, it has been found that numerical solutions show a quite good agreement in the laminar and transitional cases and a very good agreement in the fully turbulent cases, but only in the case of the more sophisticated k–ϵ turbulence model.

The necessity of using a k–ϵ turbulence model is, therefore, confirmed by this study, together to the choice of the correct laminar to turbulence transition onset (an extended transition region seems to be closer to the physics). The maximum heat flux level is, however, predicted with laminar to turbulence transition set just downstream of the hinge location and is in agreement with experiments, thus confirming the transition downstream of the reattachment.

In conclusion, further improvements of the experimental techniques and numerical methodologies seem to be necessary to correctly describe the physics of the shock-wave/boundary-layer interaction phenomena in both transitional and turbulent regimes. In particular, a more sophisticated description of the temperature along the body may be necessary. A boundary condition taking into account the whole heat transfer process on the wall should improve the numerical results.

References

[1] Stojanowski, M., and Hakenesch, P., "Mesures des flux thermiques avec des thermocouples sur la maquette no. 3042 au $\frac{1}{40}$ dans la soufflerie S4 Modane à Mach 10," European Space Agency and Dassault Aviation, Rept. H.RE.1.1114 AMD, St. Cloud, France, Nov. 1992.

[2] Stojanowski, M., "Mesures des flux thermiques par la mèthode Thermocolor sur la forme Hermes A en ecoulement hypersonique froid à Mach 10 dans la soufflerie S4 Modane," European Space Agency and Dassault Aviation, Rept. H.RE.1.1131 AMD, St. Cloud, France, Nov. 1993.

[3] Chalot, F., Mallet, M., and Ravachol, M., "A Comprehensive Finite Element Navier–Stokes Solver for Low and High Speed Aircraft Design," AIAA Paper 94-0814, Jan. 1994.

[4] Perrier, P., "Hermes, Theoretical Aerothermodynamic Report of Level 3," European Space Agency and Dassault Aviation, Rept. H.NT.1.1379 AMD, St. Cloud, France, March 1994.

[5] Pandolfi, M., "On the Flux Difference Splitting Formulation," *Notes on Numerical Fluid Mechanics*, Vol. 24, Vieweg, Braunschweig, Germany, 1989.

[6] Borrelli, S., and Pandolfi, M., "An Upwind Formulation for the Numerical Prediction of Non Equilibrium Hypersonic Flows," 12th International Conf. on Numerical Methods in Fluid Dynamics, Oxford, England, UK, July 1990.

[7] Borrelli, S., Leone, G., Marini, M., and Schettino, A., "Contributions to Cold and Hot Hyperboloid Flare Problem," 4th European High-Velocity

Database Workshop, European Space Research and Technology Center (ESTEC), CIRA-TN-95-0004, Noordwijk, The Netherlands, Nov. 1994.

[8]Marini, M., "A Contribution to T2-95 Hyperboloid Flare Problem," 1st U.S.–Europe High Speed Flow Field Database Workshop, Univ. of Houston, CIRA-TN-95-151, Houston, TX, Nov. 1995.

[9]Schettino, A., and Borrelli, S., "A Contribution to T1-95 ONERA-F4 Nozzle Problem," 1st U.S.–Europe High Speed Flow Field Database Workshop, Univ. of Houston, CIRA-TN-96-009, Houston, TX, Nov. 1995.

[10]Diurno, W. G., and Marini, M., "A Contribution to T3-95 Shock-Shock Interaction Problem," 1st U.S.–Europe High Speed Flow Field Database Workshop, Univ. of Houston, CIRA-TN-95-150, Houston, TX, Nov. 1995.

[11]Schettino, A., Borrelli, S., and De Filippis, F., "Influence of Transport and Thermokinetic Models in Free-flight and in Plasma Wind Tunnel Tests," *Proceedings of the International Symposium on Computational Fluid Dynamics*, Vol. 3, Sendai, Japan, 1993, pp. 75–80.

[12]De Filippis, F., and Borrelli, S., "Analysis of Different Approximation Levels Introduced in the Developments for Transport Coefficients Models of High Energy Air," *ICAS 94 Proceedings*, Vol. 1, International Council of the Aeronautical Sciences, Anaheim, CA, pp. 398–405 (Paper ICAS-94-2. 2.2).

[13]Baldwin, B. S., and Lomax, H., "Thin-Layer Approximation and Algebraic Model for Separated Turbulent Flows," AIAA Paper 78-257, Jan. 1978.

[14]Needham, D. A., and Stollery, J. L., "Boundary-Layer Separation in Hypersonic Flow," AIAA Paper 66-455, June 1966.

[15]Simeonides, G., "Hypersonic Shock Wave Boundary Layer Interactions over Simplified Deflected Control Surface Configurations," AGARD-FDP/VKI Special Course, AGARD Rept. R-792, Paper 7, Rhode St-Genese, Belgium, May 1993.

J. R. Maus
Associate Editor